ELSEVIER

Formation of solid and hollow cuprous oxide nanocubes in water-in-oil microemulsions controlled by the yield of hydrated electrons

Qingde Chen, Xinghai Shen [*], Hongcheng Gao

*Beijing National Laboratory for Molecular Sciences, Department of Applied Chemistry, College of Chemistry and Molecular Engineering,
Peking University, Beijing 100871, People's Republic of China*

Abstract

A local ordered structure constructed from solid Cu_2O nanocubes was obtained by the radiolytic reduction of $Cu(NO_3)_2$ in a water-in-oil (W/O) microemulsion composed of Triton X-100, n-hexanol, cyclohexane, and water in the presence of ethylene glycol (EG). However, when Triton X-100 was replaced with Brij 56 in the microemulsion, hollow Cu_2O nanocubes were synthesized. The addition of toluene into the Brij 56 system could decrease the ratio of hollow nanocubes. It was suggested that the balance between the reduction rate of Cu^{2+} depending on the yield of hydrated electrons (e_{aq}^-) and the escape rate of the mixed solvent determined their final morphologies. The presence of EG influenced the rigidity of the interface of the microemulsion and thus the above balance, which resulted in the different morphologies of Cu_2O nanoparticles in the Brij 56-based microemulsion.

© 2007 Elsevier Inc. All rights reserved.

1. Introduction

In the field of nanoscience and nanotechnology, the largest activity has been focused on the synthesis of new nanoparticles with different sizes and new shapes, which have strong effects on their widely varying properties [1,2]. Among the numerous materials, hollow materials with nanometer-to-micrometer dimensions have attracted much attention for their tailored structural, optical, mechanical, and surface properties and therefore their wide range of potential applications, such as controlled delivery, photonic crystals, fillers, and catalysts [3–8]. So far, many methods have been explored to synthesize hollow materials: "hard templates" (polystyrene spheres [3–5], silica spheres [6], metal nanoparticles [7,9], carbon nanotubes [10], etc.), "soft templates" (normal micelles [8,11,12], block copolymer micelles [13,14], polymer [15,16], microemulsions [17], etc.), in situ templates [18], and template-free methods [19–21]. However, most efforts have been made

to synthesize hollow spheres [3–7,9,13,15,16,18,20] and nanotubes [7,10,14,16,20]. There are only a few reports on hollow nanocubes [7,8,11,21,22].

γ-Irradiation has been widely used in preparing nanoparticles [23,24]. Now, there are several reports about the synthesis of hollow structures via this method [17,25,26]. However, they are limited to hollow spheres. In our previous work, we reported that the radiolytic reduction of Cu^{2+} in W/O microemulsions was well controlled by adjusting the yield of hydrated electrons (e_{aq}^-) [27]. Meanwhile, we found that it should be possible to control the shape of nanoparticles in the same way [27]. To get deep insight into this issue, it is necessary to choose two similar systems in which the yield of e_{aq}^- is obviously different, whereas other effects are identical to a great extent. For this purpose, Triton X-100 and Brij 56, whose structures are similar, were selected to construct W/O microemulsions with n-hexanol, cyclohexane, and water in the presence of ethylene glycol (EG). In the present paper, the radiolytic syntheses of solid and hollow Cu_2O nanocubes in these microemulsions are reported. It was suggested that the different morphologies of Cu_2O nanoparticles were mainly determined by the balance be-

* Corresponding author. Fax: +86 10 62759191.
  E-mail address: xshen@pku.edu.cn (X. Shen).
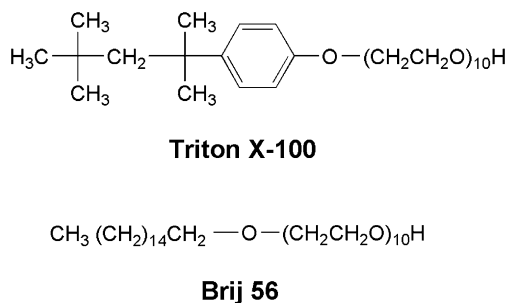
Fig. 1. Chemical structures of Triton X-100 and Brij 56.

tween the reduction rate of Cu^{2+} depending on the yield of e_{aq}^- and the escape rate of the mixed solvent.

2. Materials and methods

2.1. Chemicals

Triton X-100 (CP, Beijing Chemical Reagents Inc.) and Brij 56 (Aldrich), as shown in Fig. 1, were used as received. Cyclohexane (AR, Beijing Chemical Reagents Inc.), toluene, ethylene glycol (EG, AR, Beijing Chemical Plant), *n*-hexanol, and copper nitrate (AR, Beijing Yili Fine Chemical Products Inc.) were used without further purification. Deionized and tridistilled water was used in the experiments.

2.2. Synthesis of nanocubes

A certain amount of $Cu(NO_3)_2$ was dissolved in the mixed solvent of EG and water (molar ratio 1:7.23) to make up a $0.02 \, mol \, L^{-1}$ stock solution. To prepare microemulsions, surfactant (Triton X-100 or Brij 56), *n*-hexanol, and cyclohexane (molar ratio 1.0:1.6:57.6) were first mixed and then a certain volume of stock solution was added, with the molar ratio of water to surfactant (ω) fixed at 6.3. The mixtures were stirred at room temperature until they became transparent. After bubbling with high-purity N_2 under anaerobic conditions, the microemulsions were irradiated in the field of a ^{60}Co γ-ray source for 16 h and 40 min, with an absorbed dosage of 40 kGy. Then, after centrifugation, orange-red precipitates and yellowish solutions were obtained.

2.3. Characterization

After irradiation, the absorption spectra were immediately recorded on a U-3010 spectrometer, with identical systems that had not been irradiated as standard. Thereafter, the samples were de-emulsified and washed with ethanol and then dispersed in ethanol. The obtained dispersion was dropped onto a carbon-coated copper grid. After the solvent was evaporated at room temperature, the transmission electron microscopy (TEM) and selected area electron diffraction (SAED) images were obtained on a JEOL JEM-200CX microscope operated at 160 kV, high-resolution TEM (HRTEM) images were obtained on a Hitachi 9000 transmission electron microscope operated at 300 kV, and scanning electron microscopy (SEM) images were obtained via

an AMARY 1910FE scanning electron microscope operated at 15 kV. The range of nanoparticle sizes was determined after measuring the dimensions of more than 500 nanoparticles based on the obtained micrographs. After the dispersed sample was deposited on a piece of glass, powder X-ray diffraction (XRD) pattern was recorded on an X'Pert PRO MPD diffractometer with Cu$K\alpha$ radiation ($\lambda = 0.15418$ nm) and an X-ray photoelectron spectrum (XPS) was collected on a Kratos Axis Ultra spectrometer with monochromatized Al$K\alpha$ radiation.

3. Results

3.1. Formation of solid nanocubes in the Triton X-100-based microemulsion

Fig. 2A (curve a) shows the UV–vis spectrum of the reduction product of $Cu(NO_3)_2$ in the Triton X-100-based microemulsion. The broad absorption with a peak at ca. 510 nm can be ascribed to the characteristic absorption of Cu_2O [12,28], suggesting the generation of Cu_2O in the irradiation course. The corresponding XRD pattern is shown in Fig. 2B (curve a). The interplanar distances calculated for (110), (111), (200), (220), and (311) from the XRD pattern match well with the standard data of cubic phase Cu_2O (JCPDS File 05-0667), confirming the formation of cubic phase Cu_2O. The fact that the (200) peak is significantly intensified suggests a preferential alignment of the (100) plane parallel to the specimen surface. The corresponding XPS analysis (curve a in Fig. 2C) shows that the kinetic energy of Cu LMM is 916.3 eV, close to the value of Cu_2O in the literature [29], which further confirms the generation of Cu_2O. Besides, the Cu LMM peak characterizing Cu(0), which is usually centered at about 918.6 eV [29], is not found in Fig. 2C (curve a), indicating the absence of metallic Cu in the reduction product. It can be seen from TEM (Fig. 3A) and SEM images (Fig. 4A) that the as-prepared products are mainly composed of nanocubes, with the edge length ranging from 80 to 120 nm. These nanocubes further construct a local ordered structure spontaneously (Fig. 3A), which can be further observed via the corresponding SEM image (Fig. 4A). The typical HRTEM image shown in Fig. 5A exhibits clear lattice fringes with *d* spacing of 0.30 nm, which corresponds to (110) reflection of the cubic Cu_2O structure, confirming the formation of crystalline Cu_2O nanoparticles. The inset of Fig. 3A is a typical SAED pattern of a related solid nanocube, which indicates a highly preferred {001} orientation texture structure. It is also noticed that additional weak diffraction rings commonly appear in the SAED patterns, arising from small nanoparticles absorbed on the surface of nanocubes, which is similar to the phenomenon reported in the literature [12]. This is revealed by the TEM image (Fig. 3C), in which we can find that a few small nanoparticles absorbed on the surfaces of the nanocubes. The corresponding HRTEM image (Fig. 5B) further exhibits individual nanoparticles and clear lattice fringes with *d* spacing of 0.25 and 0.30 nm, corresponding to (111) and (110) reflections of the cubic Cu_2O structure, respectively.
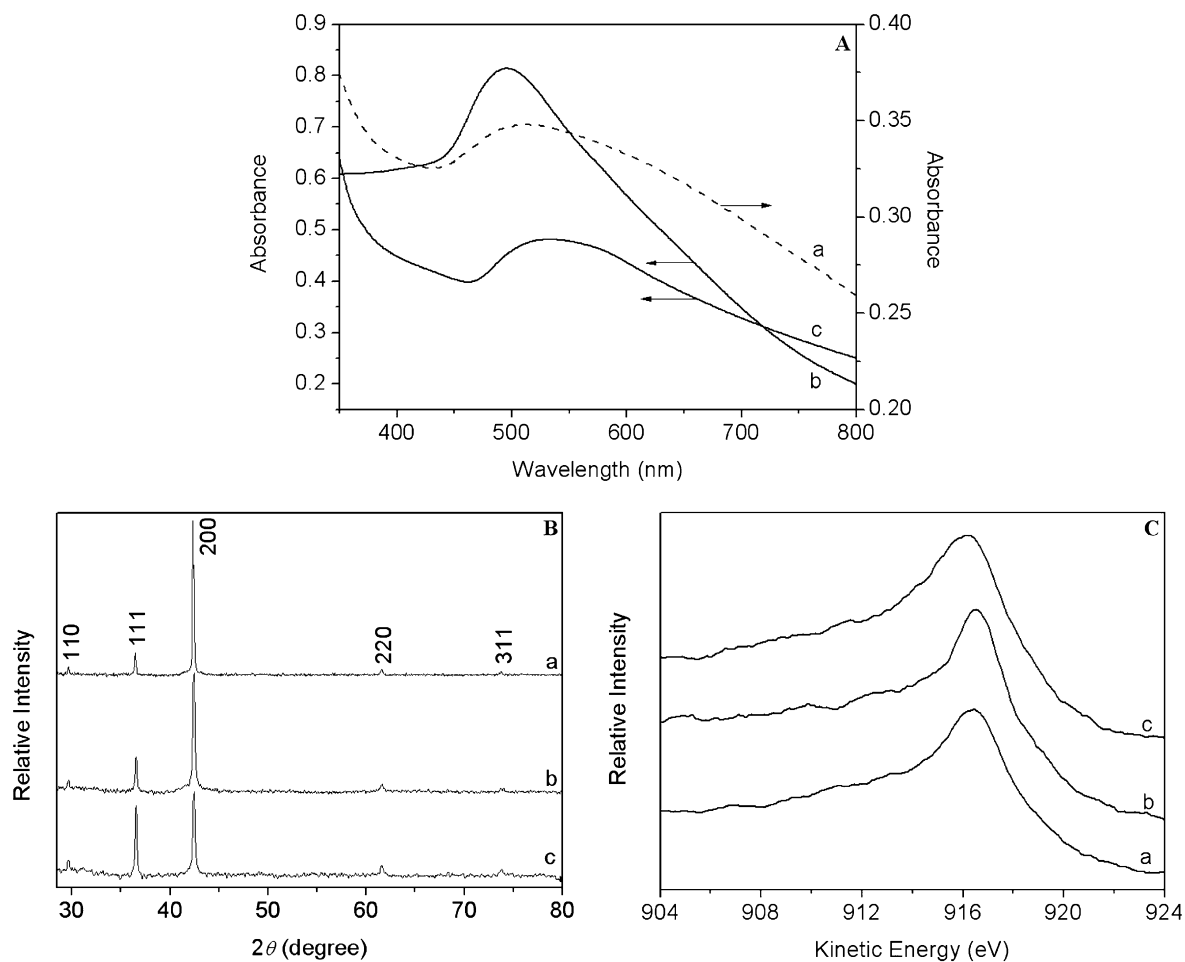
Fig. 2. UV–vis spectra (A), XRD patterns (B), and Cu LMM Auger spectra (C) of the reduction products of $Cu(NO_3)_2$ in the Triton X-100-based microemulsion (a), and in the Brij 56-based microemulsions in the absence (b), and presence (c) of toluene ([toluene] $= 1.86$ mol L^{-1}).
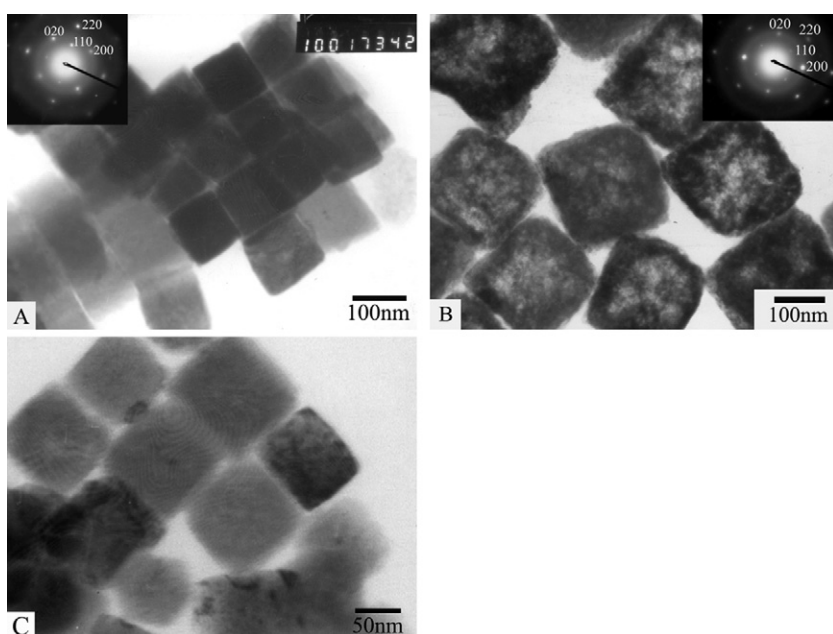
Fig. 3. TEM images of the reduction products of $Cu(NO_3)_2$ in the Triton X-100-based (A, C) or Brij 56-based (B) microemulsions. The inset shows the SAED pattern of the corresponding product.
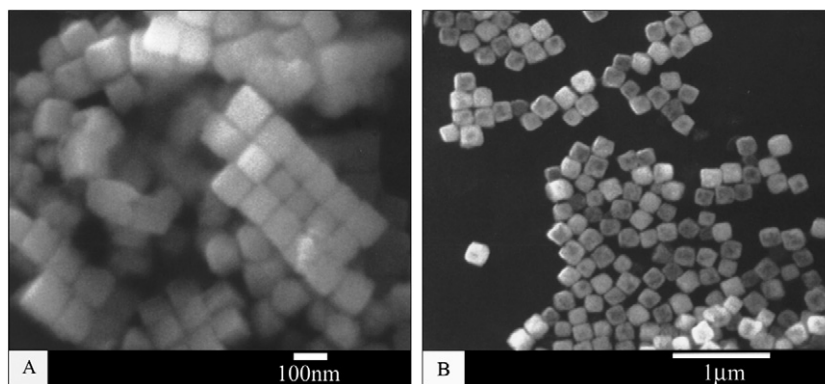
Fig. 4. SEM images of the reduction products of $Cu(NO_3)_2$ in the Triton X-100-based (A) or Brij 56-based (B) microemulsions.
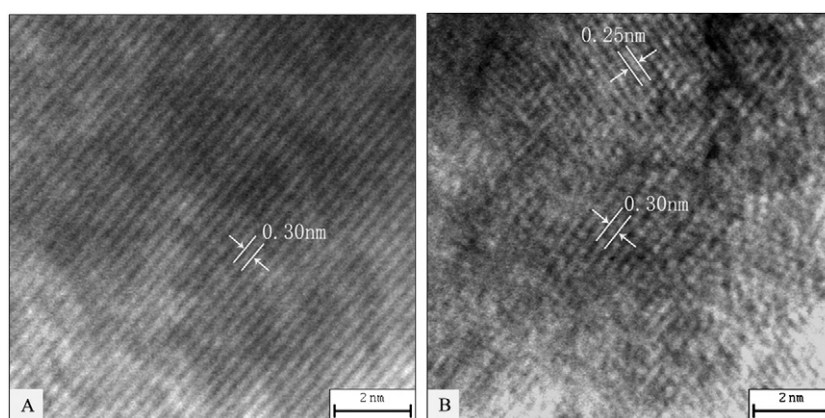
Fig. 5. HRTEM images of the reduction product of $Cu(NO_3)_2$ in the Triton X-100-based microemulsion.

3.2. Formation of hollow nanocubes in the Brij 56-based microemulsion

When Triton X-100 was replaced with Brij 56 in the microemulsion, a similar UV–vis spectrum (curve b in Fig. 2A), XRD pattern (curve b in Fig. 2B), Cu LMM Auger spectrum (curve b in Fig. 2C), SAED pattern (inset, Fig. 3B), and HRTEM images (not shown) were obtained, indicating the generation of Cu_2O nanoparticles. The corresponding TEM (Fig. 3B) and SEM (Fig. 4B) images show that the edge length of the nanocubes ranges from 130 to 210 nm. In addition, the TEM image (Fig. 3B) shows a distinct contrast between the dark edge and the pale center in most nanocubes, evidencing their hollow nature. The wall thickness is estimated to be 20–50 nm. In the absorption spectrum, the broad absorption peak is blue-shifted to about 495 nm. As is well known, the absorption band of nanoparticles is affected by the quantum size effect (QSE) [1,28]. If the QSE is related to the size of the edge length as solid nanoparticles, the hollow particles are too large to observe an obvious QSE. It may be the thickness of the hollow Cu_2O nanocubes' wall that is related to QSE, which causes the blue shift of the Cu_2O absorption peak.

3.3. Effect of toluene

It is strange that the morphologies of the reduction products of $Cu(NO_3)_2$ in the two microemulsions are markedly different, although the structures of the two nonionic surfactants are similar. After examination of their molecular structures, it can easily be found that a phenyl ring exists in the hydrophobic chain of Triton X-100. It was reported that toluene can react with the excess electrons in cyclohexane, with a rate constant of $4.0 \times 10^9 \, \mathrm{L\,mol^{-1}\,s^{-1}}$ [30]. According to this fact, it is believed that Triton X-100 can scavenge excess electrons in the oil phase (e_{oil}^-). This has been verified in our previous work [27]. To further explore the effect of the phenyl ring in this work, $1.86 \, \mathrm{mol\,L^{-1}}$ toluene was added to the Brij 56-based microemulsion, while the total volume was not changed. A similar UV–vis spectrum is obtained, but the broad absorption peak is red shifted to about 530 nm (curve c in Fig. 2A). The related TEM image (Fig. 6) shows that most nanoparticles are solid and a lot of them are constructed from small nanocubes. The related XRD pattern (curve c in Fig. 2B), Cu LMM Auger spectrum (curve c in Fig. 2C), and SAED analysis (inset, Fig. 6) confirm the formation of Cu_2O nanoparticles. There also appears serious trailing of diffraction spots in the SAED pattern, characteristic of polycrystals (see the arrowheads in the inset of Fig. 6).
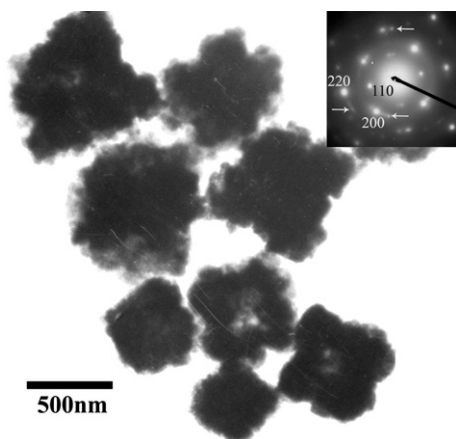
Fig. 6. TEM image of the reduction product of $Cu(NO_3)_2$ in the Brij 56-based microemulsion in the presence of toluene (1.86 mol L^{-1}). The inset shows the SAED pattern.

4. Discussion

In the radiolytic reduction of Cu^{2+}, e_{aq}^- plays the main role. First, e_{aq}^- reduces Cu^{2+} to Cu^+:

$$Cu^{2+} + e_{aq}^- \longrightarrow Cu^+. \tag{1}$$

Then, Cu_2O is generated through the hydrolysis of Cu^+:

$$Cu^+ + H_2O \longrightarrow CuOH + H^+,$$
$$2CuOH \longrightarrow Cu_2O + H_2O. \tag{2}$$
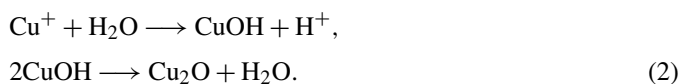
At the same time, the disproportionation,

$$2Cu^+ \longrightarrow Cu + Cu^{2+}, \tag{3}$$

and the further reduction,

$$Cu^+ + e_{aq}^- \longrightarrow Cu, \tag{4}$$

of Cu^+ are two important competing reactions, which can be suppressed by reducing the yield of e_{aq}^- [27]. During the irradiation of microemulsions, e_{aq}^- can be generated mainly from the scavenging of excess electrons, which are produced originally through the radiolysis of oil, by the water pool [27,31–34]. In addition, the radiolysis of water in the water pool can generate e_{aq}^- directly, but it is less important [27,31–34].

According to the results in the literature [31–38] and in our previous work [27], the ω value, the kind of anion, the viscosity of the water pool, and the aromatic ring can affect the yield and/or the reactivity of e_{aq}^- as follows.

(a) The yield of e_{aq}^- increases with increasing ω in W/O microemulsions not based on cationic surfactant [31–36].
(b) It is well known that NO_3^- can effectively react with e_{aq}^- in aqueous solutions, with a rate constant of 9.7×10^9 L mol^{-1} s^{-1} [37]. A similar reaction can take place in AOT-based microemulsions [36]. Thus, when NO_3^- exists in the system, the yield of e_{aq}^- will be reduced remarkably, which is propitious for the generation of Cu_2O [27].

Table 1
Comparison of the morphologies of Cu_2O nanoparticles synthesized in the Triton X-100- and Brij 56-based microemulsions both with and without EG

Surfactant	Without EG	With EG
Triton X-100	Octahedron nanocrystal, solid [28]	Nanocube, solid
Brij 56	Nanocube, solid [27]	Nanocube, hollow

(c) The presence of EG can obviously increase the viscosity of the water pool of a microemulsion. It was reported that in the AOT-based W/O microemulsion, the reactivity of e_{aq}^- could be reduced by an increase in the viscosity of the water pool [38].
(d) If e_{oil}^- is scavenged by some groups during its migration into the water pool, e.g., the phenyl ring in the hydrophobic chain of Triton X-100, the yield of e_{aq}^- is reduced, which favors the formation of Cu_2O [27].

In the two systems of this work, the effects of the ω value and NO_3^- on the yield of e_{aq}^- and the effect of EG on the viscosity of the water pool should be similar to a great extent, because the components, except the surfactant, and their contents of the two microemulsions are the same. The obvious difference should arise mainly from the effect of the phenyl ring in Triton X-100. Therefore, it is suggested here that the yield of e_{aq}^- induces the different morphologies of Cu_2O in the two systems. This is further supported by the effect of toluene.

Luo et al. [22] have obtained hollow Cu_2O nanocubes in simple solution-phase reduction systems using Triton X-100 as solvent in the presence of a small amount of ethanol. They suggested that the polyoxyethylene chain of Triton X-100 molecules could interact with ethanol via hydrogen bonds. During the ripening process, ethanol would gradually escape while the primary particles of Cu_2O were generated. The spaces of the interior enlarged with the escape of ethanol, and hollow nanocubes were finally produced [22]. Here, we suggest that in the Brij 56-based microemulsion, due to the absence of a phenyl ring, the yield of e_{aq}^- and its generation rate are higher than those in the Triton X-100-based microemulsion. Thus, the mixed solvent could not escape as soon as possible and may be encapsulated in the interior of the generated Cu_2O nanoparticles. During the process of ripening or post-treatment, the encapsulated solvent would gradually escape, leading to the formation of a hollow structure. It seems reasonable to conclude that the balance between the reduction rate of Cu^{2+} depending on the yield of e_{aq}^- and the escape rate of the mixed solvent in the water pool determines the final morphology of Cu_2O in the above two systems.

To further study the formation mechanism of hollow and solid Cu_2O nanocubes, we compare the morphologies of Cu_2O nanoparticles synthesized in the two microemulsions both with and without EG on the condition that the volume and the concentration of the added $Cu(NO_3)_2$ solutions are identical. All the results are listed in Table 1. It can easily be found that in the Brij 56-based microemulsions the obtained Cu_2O nanocubes are hollow and solid [27] in the presence and absence of EG, respectively. It is estimated that the molar ratio of Cu^{2+} to surfactant is 1:309 in this system. Then, one can suppose that a

very small number, e.g., 1–3, of copper ions exist in each water pool, depending on the average aggregation number of the surfactant. Thus, the growth of Cu_2O nanoparticles must experience a mass exchange course between water pools. The presence of EG can reduce the rigidity of the interface of a W/O microemulsion [39], similarly to the action of short-chain alcohol [40] and benzyl alcohol [40,41]. This will favor the above-mentioned mass exchange. In the Brij 56-based microemulsion with EG, although the reactivity of e_{aq}^- is reduced to a certain extent, the rate of mass exchange between water pools is increased. It might be the latter effect that plays an important role, enhancing the growth rate of Cu_2O nanoparticles and leading to the formation of hollow nanocubes. In contrast, solid nanocubes are finally formed in the Brij 56-based microemulsion without EG. However, in the Triton X-100-based microemulsions, the addition of EG only makes the morphology of Cu_2O change from octahedral nanocrystals to nanocubes. Although the rigidity of the interface is reduced in the presence of EG, the yield of e_{aq}^- and its generation rate in this system are so low that the polar solvent can escape in time. This may be the reason that the nanocubes are solid despite of the existence of EG.

Celik and Dag [42] have shown that the polyoxyethylene chain of $C_{12}H_{25}(OCH_2CH_2)_{10}OH$ can form hydrogen bonds with transition metal aqua complexes. Based on this result, it can be inferred that the polyoxyethylene chains in Triton X-100 and Brij 56 can effectively coordinate Cu^{2+} and Cu^+, and therefore the reduction of Cu^{2+} and the generation of Cu_2O take place at the interface of the microemulsions. In addition, it is noted that for the systems of pure polystyrene (PS), magnetite-coated PS with diethylene glycol (DEG), magnetite-coated PS, and magnetite nanoparticles, Huang and Tang [43] suggested that DEG could adsorb onto magnetite-coated PS and the hydroxyl groups of DEG were preferentially located within the surface region of magnetite nanoparticles. Here, EG and surfactant may also adsorb onto the special surface of the Cu_2O crystal nucleus together, affecting the growth of nanoparticles. Combining the above discussions, it can be concluded that during each step of the formation of Cu_2O nanoparticles, e.g., the reduction of Cu^{2+}, the mass exchange between water pools, and the growth of Cu_2O nanoparticles, EG plays an important role.

5. Conclusions

A local ordered structure constructed from solid Cu_2O nanocubes was obtained by the radiolytic reduction of $Cu(NO_3)_2$ in a W/O microemulsion composed of Triton X-100, n-hexanol, cyclohexane, and water in the presence of EG. However, when Triton X-100 was replaced with Brij 56 in the W/O microemulsion, hollow Cu_2O nanocubes were synthesized. The addition of toluene into the Brij 56 system could decrease the ratio of hollow nanocubes. It was suggested that the balance between the reduction rate of Cu^{2+} depending on the yield of e_{aq}^- and the escape rate of the mixed solvent determined their final morphologies. The existence of EG influenced the rigidity of the interface of the microemulsion and thus the above balance, which resulted in the different morphologies of Cu_2O nanoparticles in the Brij 56-based microemulsion. Thus, this work further demonstrates that the combination of γ-irradiation and W/O microemulsion can afford us more unique conditions to control the synthesis of nanoparticles than the routine chemical method in a microemulsion. Our results strongly suggest that the compounds with aromatic rings can be used to control the morphology of nanoparticles, which is impossible in routine chemical methods. It is also believed that the results reported herein will contribute in a new way to the synthesis of nanoparticles.

References

[1] C. Burda, X.B. Chen, R. Narayanan, M.A. El-Sayed, Chem. Rev. 105 (2005) 1025.
[2] A.P. Alivisatos, Science 271 (1996) 933.
[3] F. Caruso, R.A. Caruso, H. Mohwald, Science 282 (1998) 1111.
[4] Z.Z. Yang, Z.W. Niu, Y.F. Lu, Z.B. Hu, C.C. Han, Angew. Chem. Int. Ed. 42 (2003) 1943.
[5] M.L. Breen, A.D. Dinsmore, R.H. Pink, S.B. Qadri, B.R. Ratna, Langmuir 17 (2001) 903.
[6] S.W. Kim, M. Kim, W.Y. Lee, T. Hyeon, J. Am. Chem. Soc. 124 (2002) 7642.
[7] Y.G. Sun, B. Mayers, Y.N. Xia, Adv. Mater. 15 (2003) 641.
[8] X.D. Li, H.S. Gao, C.J. Murphy, L.F. Gou, Nano Lett. 4 (2004) 1903.
[9] Y.D. Jin, S.J. Dong, J. Phys. Chem. B 107 (2003) 12902.
[10] P.M. Ajayan, O. Stephan, P. Redlich, C. Colliex, Nature 375 (1995) 564.
[11] L.F. Gou, C.J. Murphy, Nano Lett. 3 (2003) 231.
[12] H.R. Zhang, C.M. Shen, S.T. Chen, Z.C. Xu, F.S. Liu, J.Q. Li, H.J. Gao, Nanotechnology 16 (2005) 267.
[13] Y.R. Ma, L.M. Qi, J.M. Ma, H.M. Cheng, W. Shen, Langmuir 19 (2003) 9079.
[14] Y.R. Ma, L.M. Qi, J.M. Ma, H.M. Cheng, Adv. Mater. 16 (2004) 1023.
[15] Y.G. Li, P. Zhou, Z.H. Dai, Z.X. Hu, P.P. Sun, J.C. Bao, New J. Chem. 30 (2006) 832.
[16] X.L. Gou, F.Y. Cheng, Y.H. Shi, L. Zhang, S.J. Peng, J. Chen, P.W. Shen, J. Am. Chem. Soc. 128 (2006) 7222.
[17] D.Z. Wu, X.W. Ge, Z.C. Zhang, M.Z. Wang, S.L. Zhang, Langmuir 20 (2004) 5192.
[18] J.J. Zhu, S. Xu, H. Wang, J.M. Zhu, H.Y. Chen, Adv. Mater. 15 (2003) 156.
[19] Q.Y. Lu, F. Gao, D.Y. Zhao, Chem. Phys. Lett. 360 (2002) 355.
[20] Y. Ni, H. Liu, F. Wang, G. Yin, J. Hong, X. Ma, Z. Xu, Appl. Phys. A 79 (2004) 2007.
[21] J.J. Teo, Y. Chang, H.C. Zeng, Langmuir 22 (2006) 7369.
[22] F. Luo, D. Wu, L. Gao, S.Y. Lian, E.B. Wang, Z.H. Kang, Y. Lan, L. Xu, J. Cryst. Growth 285 (2005) 534.
[23] A. Henglein, J. Phys. Chem. 97 (1993) 5457.
[24] J. Belloni, M. Mostafavi, H. Remita, J.L. Marignier, M.O. Delcourt, New J. Chem. 22 (1998) 1239.
[25] Y. Hu, J.F. Chen, W.M. Chen, X.H. Lin, X.L. Li, Adv. Mater. 15 (2003) 726.

[26] J.X. Huang, Y. Xie, B. Li, Y. Liu, Y.T. Qian, S.Y. Zhang, Adv. Mater. 12 (2000) 808.

[27] Q.D. Chen, X.H. Shen, H.C. Gao, J. Colloid Interface Sci. 308 (2007) 491.

[28] P. He, X.H. Shen, H.C. Gao, J. Colloid Interface Sci. 284 (2005) 510.

[29] J.F. Moulder, W.F. Stickle, P.E. Sobol, K.D. Bomben, Handbook of X-ray Photoelectron Spectroscopy, Perkin–Elmer Physical Electronics Division, Eden, 1992, p. 203.

[30] V.I. Tupikov, in: V.K. Milinchuk, V.I. Tupikov (Eds.), Organic Radiation Chemistry Handbook, Ellis Horwood Ltd. Chichester, 1989, p. 46.

[31] M. Wong, M. Gratzel, J.K. Thomas, Chem. Phys. Lett. 30 (1975) 329.

[32] J.L. Gebicki, L. Gebicka, J. Kroh, J. Chem. Soc. Faraday Trans. 90 (1994) 3411.

[33] S. Adhikari, R. Joshi, C. Gopinathan, J. Colloid Interface Sci. 191 (1997) 268.

[34] R. Joshi, T. Mukherjee, Radiat. Phys. Chem. 66 (2003) 397.

[35] M.P. Pileni, B. Hickel, C. Ferradini, J. Pucheault, Chem. Phys. Lett. 92 (1982) 308.

[36] M.P. Pileni, P. Brochette, B. Hickel, B. Lerebours, J. Colloid Interface Sci. 98 (1984) 549.

[37] G.V. Buxton, C.L. Greenstock, W.P. Helman, A.B. Ross, J. Phys. Chem. Ref. Data 17 (1988) 513.

[38] V. Calvo-Perez, G.S. Beddard, J.H. Fendler, J. Phys. Chem. 85 (1981) 2316.

[39] L. Garcia-Rio, J.R. Leis, J.C. Mejuto, M.E. Pena, E. Iglesias, Langmuir 10 (1994) 1676.

[40] S. Modes, P. Lianos, J. Phys. Chem. 93 (1989) 5854.

[41] R.P. Bagwe, K.C. Khilar, Langmuir 13 (1997) 6432.

[42] O. Celik, O. Dag, Angew. Chem. Int. Ed. 40 (2001) 3799.

[43] Z.B. Huang, F.Q. Tang, J. Colloid Interface Sci. 275 (2004) 142.